Design, fabrication, and characterization of thermoplastic microlenses for fiber-optic probe imaging

Shinoj, V. K.; Murukeshan, V. M.; Tor, S. B.; Loh, N. H.; Lye, S. W.

2014

Shinoj, V. K., Murukeshan, V. M., Tor, S. B., Loh, N. H., & Lye, S. W. (2014). Design, fabrication, and characterization of thermoplastic microlenses for fiber-optic probe imaging. Applied Optics, 53(6), 1083-1088.

https://hdl.handle.net/10356/98860

https://doi.org/10.1364/AO.53.001083

Design, fabrication, and characterization of thermoplastic microlenses for fiber-optic probe imaging

V. K. Shinoj,[1,*] V. M. Murukeshan,[1] S. B. Tor,[1,2] N. H. Loh,[1] and S. W. Lye[1]

[1]Center for Optical and Laser Engineering (COLE), School of Mechanical and Aerospace Engineering, Nanyang Technological University, Nanyang Avenue, Singapore 639798

[2]Singapore-MIT Alliance (SMA), N3.2-01-36, 65 Nanyang Drive, Singapore 637460

*Corresponding author: shinoj@ntu.edu.sg

Received 21 October 2013; accepted 6 January 2014;
posted 24 January 2014 (Doc. ID 199852); published 13 February 2014

Microlens-ended fibers could find great usefulness in future biomedical applications, particularly in endoscopic imaging applications. In this context, this paper focuses on microlens-attached specialty optical fibers such as imaging fiber that can be used for probe imaging applications. Stand-alone self-aligned polymer microlenses have been fabricated by microcompression molding. The fabrication parameters have been optimized for different materials, such as poly(methyl methacrylate) (PMMA), polycarbonate (PC Lexan 123R), Zeonor 1060R (ZNR), and Topas COC. A comparison study of the focusing and spatial resolution of the fabricated lenses is performed prior to employing them for fiber-optic fluorescence imaging applications.

OCIS codes: (110.2350) Fiber optics imaging; (080.3620) Lens system design; (170.2150) Endoscopic imaging; (170.2520) Fluorescence microscopy.
http://dx.doi.org/10.1364/AO.53.001083

1. Introduction

Fiber-optic probes are generally used for performing *in vivo* optical imaging of internal tissues because of their smaller size and flexibility [1]. The main components of such a fiber-optic probe system are a small lens and a beam director, which provide a focused optical beam directed to a region of interest. Many studies of the microlens-ended fiber probes have been reported in the recent years [2–5]. In many cases, a conventional microball lens is microassembled and glued in the V-groove in various fiber-optic applications [6,7]. However, the gluing of a microlens to the fiber tip is a cumbersome and expensive process that often results in a low-quality optical interface [2]. The fabrication of microimaging lenses on the top of imaging fibers by the direct lithographic and laser-micro furnace techniques was also investigated [8,9]. The fabrication procedure is quite complex and time consuming, and it is hard to control the size and position of a microlens. The mounting of a microlens is effected on a built-in concave cone-etched single-mode fiber [10]. However, the fiber preparation procedures are quite cumbersome, and they are difficult in the case of fiber with multiple cores as in the case of image fiber bundles that have small, closely spaced cores.

Thermoplastic polymers have become popular over glass as material for optical devices due to their lower cost, lightness, and ease of processing [11]. Design and fabrication of stand-alone thermoplastic polymer microlenses through compression molding have been reported recently by our group [12–14]. In this paper, we compare the performance of lenses made of different thermoplastic polymer materials to

1559-128X/14/061083-06$15.00/0

find the best polymer microlens for subsequent application in our fiber-optic probe imaging scheme.

2. Choice of Lens Materials and Fabrication Process

Thermoplastic polymers differ in cost and also in physical properties, such as glass transition temperature and melting point. The physical properties will behave differently under different molding sequences and parameters. In this paper, the property and feasibility of four thermoplastic polymers—poly(methyl methacrylate) (PMMA), polycarbonate (PC), Zeonor 1060R (ZNR), and Topas COC—will be discussed. Zeonor and Topas belong to the family of cyclic olefin copolymers (COCs), which possess a higher glass transition temperature and a higher optical transmission compared to PMMA and PC. Polymers that come in pellet form are extruded into long filaments using an extrusion process and then cut into smaller cylindrical gobs for the final molding into microlenses. Please refer to our previous papers [13,14] for a detailed description of the fabrication process.

In this research, a Taguchi L-type orthogonal array was chosen to analyze the effects of different factors, such as molding temperature, demolding temperature, and holding time, for each process on the surface roughness and the radius of the lenses. The combination of these factors will be tested to find the best parameters in producing microlenses. A high value of signal-to-noise ratio (S/N) stands for a higher level of effect of the corresponding factor, whereas a low S/N corresponds to a lower effect of the corresponding factor [15]. The optimized parameters are derived from the maximum S/N and the mean value of surface roughness results meeting the optimum condition. An overview of the optimized parameters of these polymer lenses is given in Table 1. Another quantitative approach to analyze the effect of the various factors in this study is through the analysis of variance (ANOVA), which considers the relative significance of the individual factors and the interaction effects [15]. Based on ANOVA table analysis, the molding temperature and holding time are seen to play a dominant role in the surface roughness of the microlens. The surface roughness of the lenses fabricated by compression molding is mainly studied using confocal microscopy and scanning electron microscopy (SEM). Confocal microscopy makes use of the optical resolution and contrast of a micrograph to eliminate out-of-focus light in specimens that are thicker than the focal plane. This allows three-dimensional structures to be reconstructed from the data. The obtained confocal images, surface plots, and SEM images of the polymer lenses with the optimized parameters given in Table 1 are as shown in Fig. 1.

3. Focal Length Measurement of Lensed Image Fiber

A. Ray Tracing Method

The lens designed and fabricated with our molding apparatus has a spherical part and a cylindrical part. The clear aperture of the lens is ≈1 mm with a total dimension of 1.4 mm including the extended side wall that enables snap fitting of the stand-alone lens on the fiber tip. The distance between the fiber outer coating and the side wall of the lens is within the tolerance limit. A schematic ray diagram for the focal length measurement of the lenses is shown in Fig. 2.

Lambda Research's TracePro (Lambda Research Corp., Littleton, Massachusetts), an existing ray tracing CAD suite, is selected to perform the required ray tracing for optimization and design iteration of the microlenses. Microlenses are designed using TracePro software for different polymers, such as PMMA, Topas, Zeonor, and PC. The dimensions of the designed microlenses are exactly the same as those of the fabricated lenses. The obtained result is shown in Fig. 3. The ray tracing option gives focal length values of 2.21, 2.203, 2.13, and 1.87 mm, respectively, for lens materials PMMA, Topas, Zeonor, and PC. The theoretical focal length value of the plano-convex microlens is estimated using the basic lens maker's formula [16]:

$$f = \frac{R}{n-1}, \tag{1}$$

where f is the lens focal length, R is the radius of curvature, and n is the refractive index of the lens. The focal lengths of the microlenses are calculated for different lens material based on the average radius of curvature given in Table 1. The calculated focal length values are 2.2, 2.21, 2.11, and 1.84 mm,

Table 1. List of Optimized Parameters Obtained from Our Lens Fabrication Procedures for Different Polymers

Polymer	Refractive Index (at 589 nm)	Holding Time (s)	Glass Transition Temperature (T_g) (°C)	Molding Temperature (°C)	Demolding Temperature (°C)	Average Radius of Curvature (μm)	Focal Length Theoretical/ Actual (mm)
Poly(methyl methacrylate) (PMMA)	1.491	45	105	135	40	1085	2.2/1.87
Polycarbonate (PC Lexan 123R)	1.586	30	130	170	50	1083	1.84/1.68
Zeonor 1060R (ZNR)	1.5309	30	139	125	60	1120	2.11/2.05
Topas COC	1.533	60	140	115	35	1179	2.21/1.98

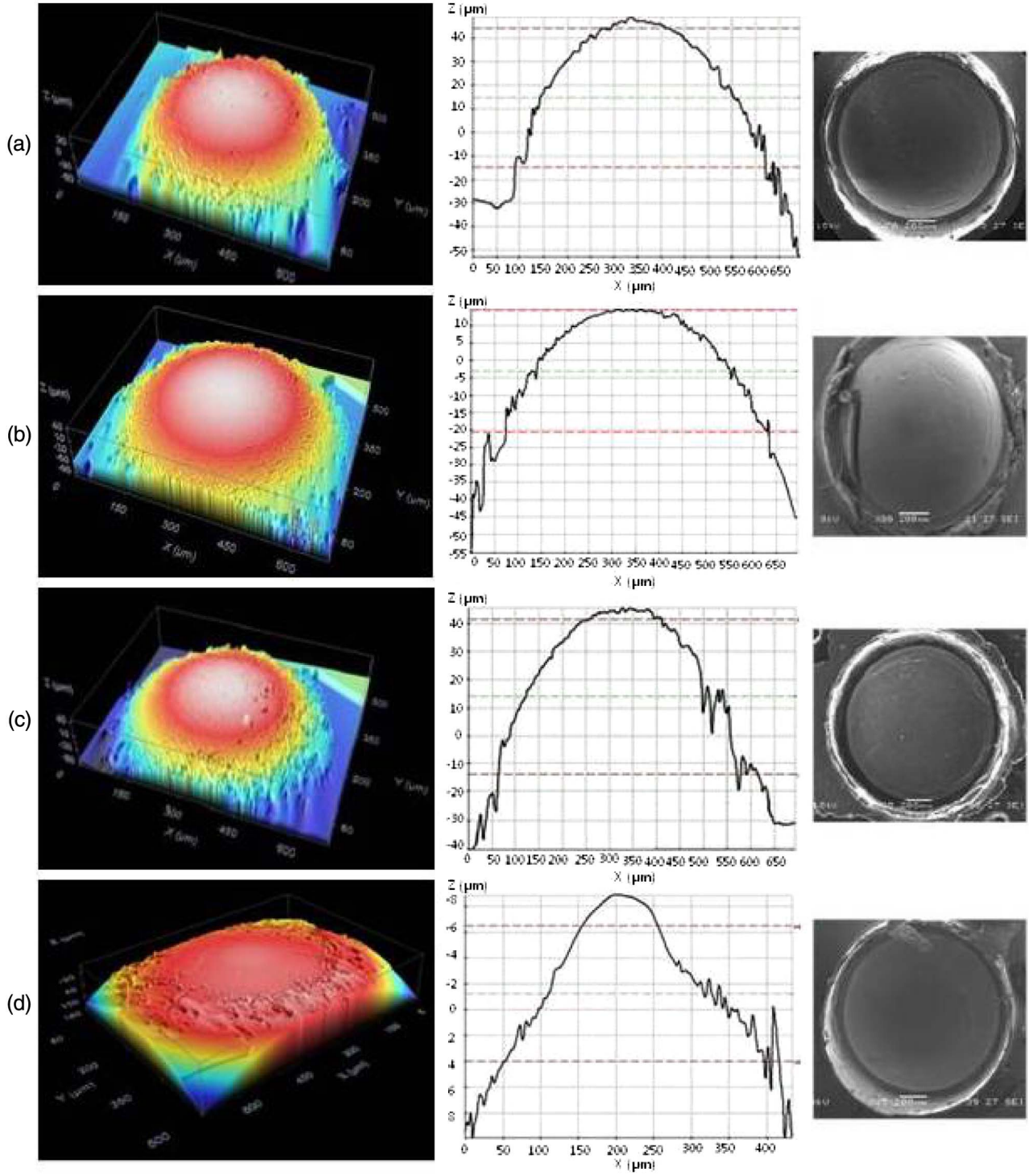

Fig. 1. Confocal image, surface profile, and SEM image of microlens made of (a) PMMA, (b) PC, (c) Zeonor, and (d) Topas.

respectively, for lens materials PMMA, Topas, Zeonor, and PC. We can see that these values strongly concur with the results obtained from the ray tracing method.

B. Experiment

The optical setup used for measuring the focal length of the fabricated microlenses is shown in Fig. 4. A collimated beam from a laser light source is focused using the fabricated microlens. An objective lens and a CCD camera integrated to a computer function as an imaging unit. The imaging unit placed on an X–Y translational stage is used for imaging the focal point and the lens surface. The imaging unit is moved horizontally to image the smallest spot of light formed by the microlens. The imaging unit is further moved to image the surface of the microlens. The distance that the precision stage travels to change the focus from

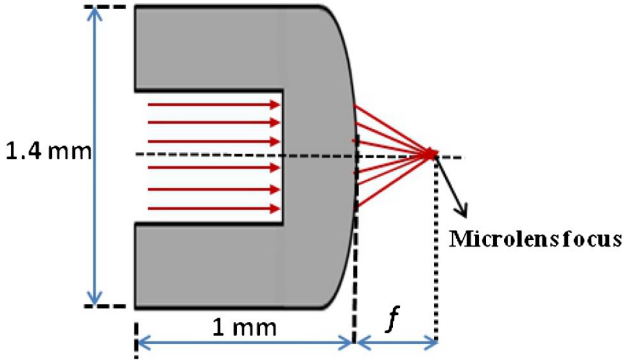

Fig. 2. Ray diagram for focal length measurement of microlens.

the focal spot to the surface of the lens is measured as the focal length. The sample images and corresponding surface plots at the focal spot and lens surface are given in Fig. 5. The obtained focal length values for lens materials PMMA, Topas, Zeonor, and PC are 1.87, 1.98, 2.05, and 1.68 mm, respectively.

The calculated theoretical values and the measured experimental values of the focal length of the microlenses are given in the last column of Table 1. The focal length values show that the molded lens can be used in fiber probe imaging applications.

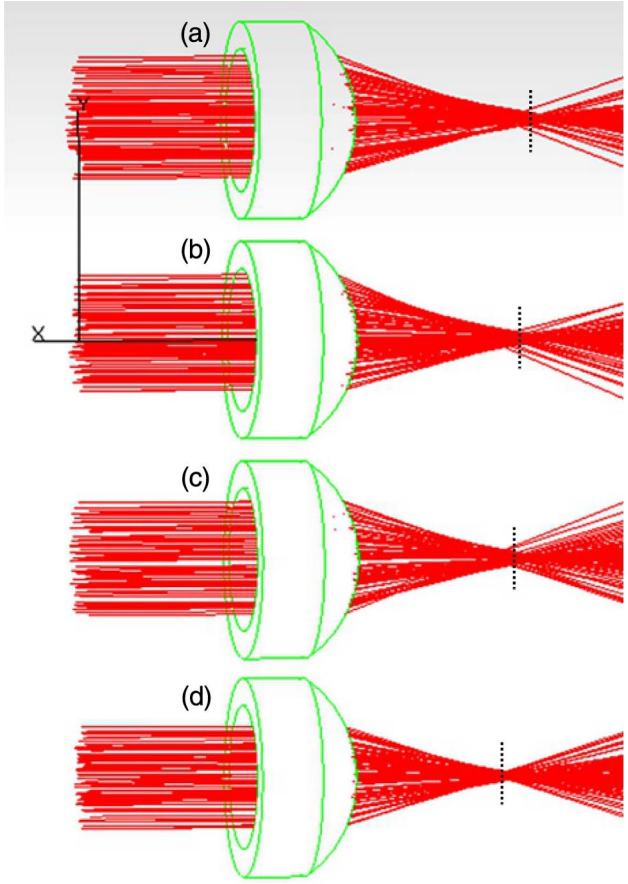

Fig. 3. Ray tracing simulation by TracePro. (a) PMMA, $f = 2.21$ mm; (b) Topas, $f = 2.203$ mm; (c) Zeonor, $f = 2.13$ mm; and (d) PC, $f = 1.87$ mm.

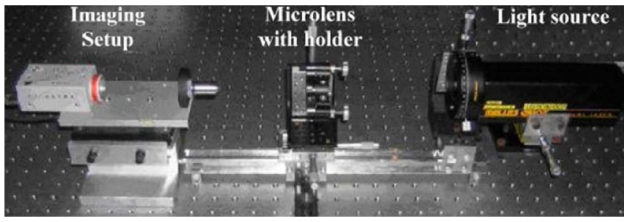

Fig. 4. Optical setup used for the focal length measurement of microlenses.

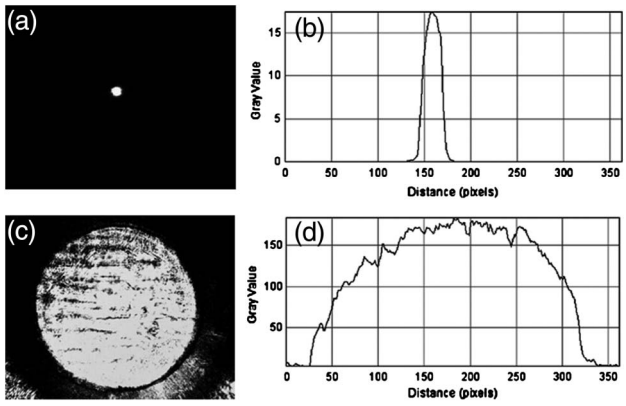

Fig. 5. CCD images and corresponding surface profiles at (a), (b) focal point and (c), (d) lens surface.

4. Fiber-Optic Probe for Fluorescence Imaging

An image fiber bundle is used in this study that has 15,000 fiberlets (fiber pixels) with a numerical aperture (NA) of 0.35 (Fujikura, 0.6 mm core diameter). A photograph of the fabricated stand-alone microlenses and microlens-tipped image fiber bundle and SEM images of the fiber are shown in Fig. 6. The actual resolution of the microlens-tipped image fiber system is characterized by the smallest feature on the resolution test chart (USAF chart) that can be resolved in the images taken using the microlens-tipped image fiber.

Figure 7(a) shows the optical setup used for this study. It consists of a collimated white light source to illuminate the test chart, the fabricated microlens-tipped image fiber bundle for the collection of signal. The image fiber bundle is coupled to a CCD camera integrated to a computer. The obtained results for different lens materials are given in Fig. 7(b). It can be seen that the smallest feature in the test chart resolvable by the image fiber system using a lens fabricated with Zeonor and Topas is the first element of the fourth group. This corresponds to a lateral resolution of ~31.25 μm. The image fiber system tipped with polycarbonate based microlens is able to resolve until element 2 of the fourth group (lateral resolution ~27.86 μm). The PMMA based microlens-tipped image fiber shows the highest resolution of ~15.63 μm (first element of fifth group). Hence, the PMMA based microlens is selected for the subsequent imaging application. The obtained resolution value of the microlens-tipped fiber-optic

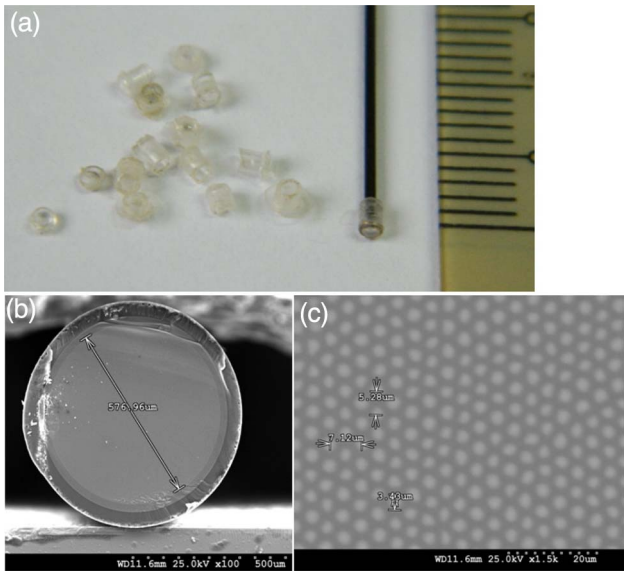

Fig. 6. (a) Photograph of fabricated stand-alone microlenses and microlens-tipped image fiber. (b), (c) SEM images of image fiber at different magnifications.

probe demonstrates the usefulness of the same in potential endoscopic applications.

The actual experimental setup is shown in Fig. 8. It consists of a coherent light source (532 nm laser), a test sample, a CCD camera connected to a computer, a beam splitter (BS), an objective lens, and an image

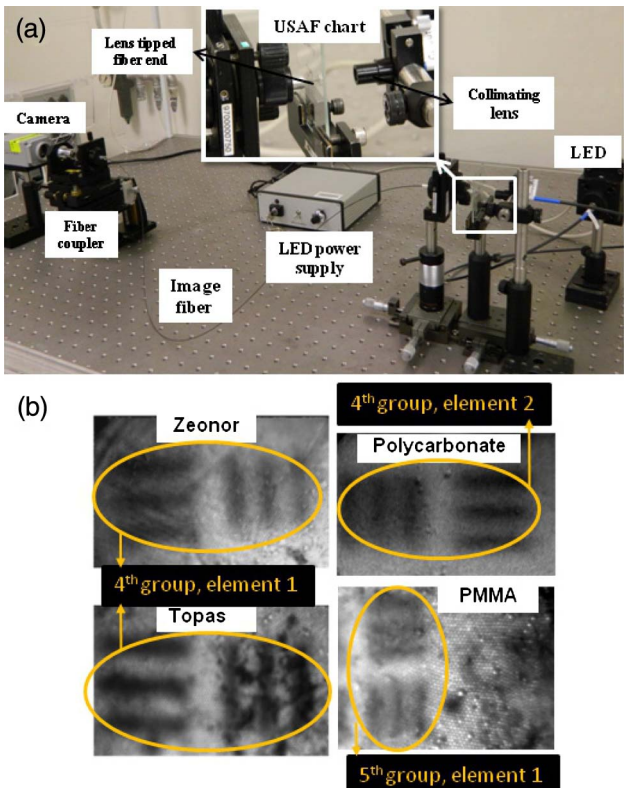

Fig. 7. (a) Photograph of experimental setup for evaluation of the resolution of microlens-attached image fiber. (b) Obtained maximum resolution for microlens made of different materials.

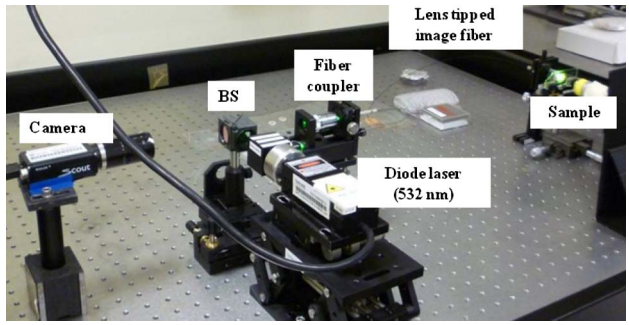

Fig. 8. Photograph of the experimental setup that simulates an endoscope.

fiber tipped with the fabricated microlens. The diverging beam from the diode laser is collimated by a lens and is directed to the fiber coupling unit (Newport F-91TS Coupler) using a dichroic BS. The microscope objective (MO) lens of the coupling unit Newport M-20×, 0.4NA is integrated with the fiber coupler at the proximal end of the image fiber. The microlens-tipped image fiber performs illumination, collection, as well as depth discrimination. The molded microlens-tipped image fiber is simulated as an endoscope probe to image the test samples, which have similar properties to the human tissues. Test samples are glass microbubbles (GMBs) from 3M Scotchlite of variable sizes (2–20 μm) embedded in a polyvinyl alcohol (PVA) matrix that simulates human tissues. A dye (Rhodamine 6G) is added as a fluorescence material in the GMB-PVA composite so that the fluorescence images of the GMBs can be highlighted. The GMB has an emission peak at 566 nm for 532 nm excitation. Figure 9 shows the images taken from different parts of the test sample. The presence of fluorescent microbubbles is visible in the obtained images.

The distance between the microlens and the fiber is adjustable as the position of the distal end of the microlens fitted to the flexible part of the probe can be changed. The micromolding process provides relatively high production rate in comparison to other microlens development techniques. The side wall of the microlens is to secure it onto the tip of the imaging fiber, and this eliminates the need for costly microassembly processes or the use of expensive gradient-index lenses.

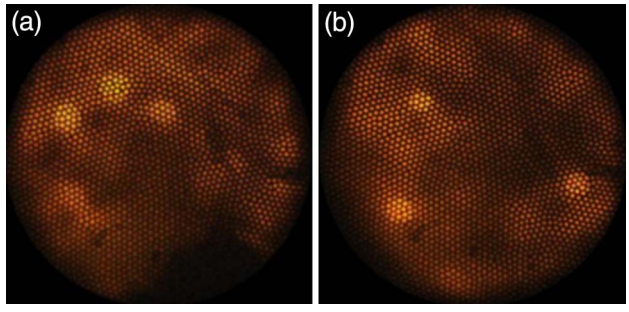

Fig. 9. (a), (b) Images of test sample taken with microlens-tipped image fiber probe system from different parts of the sample.

5. Conclusions

The optimum parameters of microlens fabrication using the microcompression molding method, such as molding temperature, demolding temperature, and holding time, are investigated for different polymer materials. The focusing ability, spatial resolution, and relevant imaging capability of these lenses in a fiber-optic probe scheme are studied. The suitability of the molded microlenses in the fiber-optic fluorescence imaging system was illustrated. The obtained results and analysis of the data indicate that the proposed embedded fiber lens based probe configurations and related methodologies can find potential biomedical diagnostics applications such as fluorescence based imaging and sensing.

V. M. M. acknowledges the financial support received through MOE AcRF (RG 10/34) and through COLE-EDB funding. The authors acknowledge the technical contribution from the following NTU students: Gary Chua Wee Min, Ong Jiong Hong, Adrian Leong Sang Jie, Zhang Ying, and Kuan Jinwei Nicodemus.

References

1. W. A. Reed, M. F. Yan, and M. J. Schnitzer, "Gradient-index fiber-optic microprobes for minimally invasive *in vivo* low-coherence interferometry," Opt. Lett. **27**, 1794–1796 (2002).
2. Y. Mao, S. Chang, S. Sherif, and C. Flueraru, "Graded-index fiber lens proposed for ultrasmall probes used in biomedical imaging," Appl. Opt. **46**, 5887–5894 (2007).
3. R. A. McLaughlin and D. D. Sampson, "Clinical applications of fiber-optic probes in optical coherence tomography," Opt. Fiber Technol. **16**, 467–475 (2010).
4. V. M. Murukeshan and N. Sujatha, "All fiber based multi-speckle modality endoscopic system for imaging medical cavities," Rev. Sci. Instrum. **78**, 053106 (2007).
5. M. V. Krishnan, M. V. Matham, S. Krishnan, P. Parasuraman, J. Joseph, and K. Bhakoo, "Red, green, and blue gray-value shift-based approach to whole-field imaging for tissue diagnostics," J. Biomed. Opt. **17**, 0760101 (2012).
6. S.-S. Lee, L.-S. Huang, C.-J. Kim, and M. C. Wu, "Free-space fiber-optic switches based on MEMS vertical torsion mirrors," J. Lightwave Technol. **17**, 7–13 (1999).
7. M.-H. Kiang, O. Solgaard, K. Y. Lau, and R. S. Muller, "Electrostatic combdrive-actuated micromirrors for laser-beam scanning and positioning," J. Microelectromech. Syst. **7**, 27–37 (1998).
8. L. G. Cohen and M. V. Schneider, "Microlenses for coupling junction lasers to optical fibers," Appl. Opt. **13**, 89–94 (1974).
9. V. Russo, G. C. Righini, S. Sottini, and S. Trigari, "Lens-ended fibers for medical applications: a new fabrication technique," Appl. Opt. **23**, 3277–3283 (1984).
10. N.-E. Demagh, A. Guessoum, R. Zegari, and T. Gharbi, "Self-centring technique for fibre optic microlens mounting using a concave cone-etched fibre," Meas. Sci. Technol. **22**, 115302 (2011).
11. K. Bescherer, D. Munzke, O. Reich, and H.-P. Loock, "Fabrication and modeling of multimode fiber lenses," Appl. Opt. **52**, B40–B45 (2013).
12. M. Mirkhalaf, S. B. Tor, V. M. Murukeshan, N. H. Loh, and S. W. Lye, "Optimization of compression molding of stand-alone microlenses: simulation and experimental results," Polym. Eng. Sci. **50**, 2216–2228 (2010).
13. M. Mirkhalaf, S. B. Tor, V. M. Murukeshan, N. H. Loh, and S. W. Lye, "Fabrication of a stand-alone polymer microlens: design of molding apparatus, simulation and experimental results," J. Micromech. Microeng. **19**, 095005 (2009).
14. M. Mirkhalaf, V. M. Murukeshan, S. Beng Tor, V. K. Shinoj, and K. Sathiyamoorthy, "Characteristics of stand-alone microlenses in fiber-based fluorescence imaging applications," Rev. Sci. Instrum. **82**, 043110 (2011).
15. R. K. Roy, *A Primer on the Taguchi Method* (Society of Manufacturing Engineers, 2010).
16. E. Hecht and A. Zajac, *Optics*, Addison-Wesley Series in Physics (Addison-Wesley, 1974).